PAPER

# Sheath and arc-column voltages in high-pressure arc discharges

J. Phys. D: Appl. Phys. **45** (2012) 355201 (10pp) doi:10.1088/0022-3727/45/35/355201

# Sheath and arc-column voltages in high-pressure arc discharges

**M S Benilov[1,3], L G Benilova[1], He-Ping Li[2,3] and Gui-Qing Wu[2]**

[1] Departamento de Física, CCCEE, Universidade da Madeira, Largo do Município, 9000 Funchal, Portugal

[2] Department of Engineering Physics, Tsinghua University, Beijing 100084, People's Republic of China

E-mail: benilov@uma.pt and liheping@tsinghua.edu.cn

Received 27 May 2012, in final form 1 July 2012
Published 14 August 2012
Online at stacks.iop.org/JPhysD/45/355201

**Abstract**

Electrical characteristics of a 1 cm-long free-burning atmospheric-pressure argon arc are calculated by means of a model taking into account the existence of a near-cathode space-charge sheath and the discrepancy between the electron and heavy-particle temperatures in the arc column. The computed arc voltage exhibits a variation with the arc current $I$ similar to the one revealed by the experiment and exceeds experimental values by no more than approximately 2 V in the current range 20–175 A. The sheath contributes about two-thirds or more of the arc voltage. The LTE model predicts a different variation of the arc voltage with $I$ and underestimates the experimental values appreciably for low currents but by no more than approximately 2 V for $I \gtrsim 120$ A. However, the latter can hardly be considered as a proof of unimportance of the space-charge sheath at high currents: the LTE model overestimates both the resistance of the bulk of the arc column and the resistance of the part of the column that is adjacent to the cathode, and this overestimation to a certain extent compensates for the neglect of the voltage drop in the sheath. Furthermore, if the latter resistance were evaluated in the framework of the LTE model in an accurate way, then the overestimation would be still much stronger and the obtained voltage would significantly exceed those observed in the experiment.

(Some figures may appear in colour only in the online journal)

## 1. Introduction

### *1.1. No-sheath versus sheath-accounted approaches to modelling of near-cathode regions of high-pressure arcs*

Theoretical description and modelling of interaction of high-pressure arc plasmas with refractory cathodes represent a topic of significant applied interest and have attracted considerable attention in the literature over the last 20 years. Two very different approaches have emerged. One group of researchers believes that space-charge effects on refractory cathodes are small and contribute to the arc voltage by no more than 1 or 2 V. Accordingly, these researchers use simulation models, which are based on the assumption of quasi-neutrality, or an even stronger assumption of local thermodynamic equilibrium (LTE), in the whole arc volume, which means neglect of all space-charge sheaths, e.g. [1–12]. Other researchers believe that the voltage drop in the near-cathode space-charge sheath is no less than 10 V and rely on models where the near-cathode sheath plays a central role (e.g. [13] and references therein; [14-16] may be cited as further examples).

Reliable experimental data on the near-cathode voltage drop in high-pressure arcs are difficult to obtain. Considerable effort has been invested over the last decade in the field of low-current arcs (arc currents $I \lesssim 10$ A), which are used, for example, in high-intensity discharge lamps. Important advances have been achieved, in particular, by Mentel and co-workers in Bochum (e.g. [17–19]; see also references in [13, 20]). Two independent methods have been used to determine the near-cathode voltage drop (cathode fall), namely electrostatic probe measurements and an analysis of the cathodic power balance based on spatially resolved measurement of the cathode surface temperature. Near-cathode voltages given by both methods agreed with each other [19, 21] and were typically in the range 10–50 V. The situation is much less favourable as far as high-current arcs ($I \gtrsim 100$ A)

[3] Author to whom any correspondence should be addressed.

 

are concerned, which are used, for example, in arc welding: the experimental data are scarce and far from being conclusive. A representative example of experimental difficulties can be found in the expert and careful work [22, p 66]: a spatial distribution of floating potential of an electrostatic probe was measured in the vicinity of a tungsten cathode of an arc in atmospheric-pressure He or Ar; when extrapolated to the cathode surface, this distribution gave the value of 4 V; the final value of 11 V for the near-cathode voltage drop was deduced by adding a voltage drop in the near-probe layer, which was estimated to be around 7 V.

The above-cited experimental values of cathode fall in low-current arcs in the range 10–50 V indicate that the first above-described (no-sheath) approach is not justified and the second (sheath-accounted) approach should be used for such arcs, and there is not much argument about it at present. An extensive comparison with the experiment on low-current arcs has convincingly validated the sheath-accounted approach (e.g. [13] and references therein; [16] is a further example). As far as high-current arcs are concerned, the above-cited experimentally derived value of the cathode fall voltage of 11 V [22, p 66] supports the second approach against the first one. However, this result can hardly play a role of the ultimate argument given the indirect character of its derivation.

The *status quo* is as follows: the approach accounting for the cathode sheath is used in most works dedicated to plasma–cathode interaction in low-current arcs; the no-sheath approach is used in most works dedicated to modelling of high-current arcs. Amazingly, there has been virtually no interaction between research in the two fields, in spite of the fact that the physics of near-cathode plasma layers in high- and low-current arcs is similar, and the question as to which approach is better physically justified for high-current arcs remains open.

### *1.2. Methodological considerations*

Given the absence of unambiguous experimental indications, it is useful to analyse the no-sheath versus sheath-accounted approaches from the point of view of methodology.

First, the sheath-accounted approach takes into account, in addition to separation of charges, all physical effects considered in the no-sheath approach, in particular, ambipolar diffusion of the charged particles. Therefore, the sheath-accounted approach is more general than the no-sheath approach, hence the former may be used to validate the latter. In other words, if the sheath-accounted approach shows that the separation of charges is a minor effect and the sheath voltage does not exceed 1 or 2 V for a certain situation, then the no-sheath approach is justified in this situation. As an example, let us consider the voltage drop $U_{\rm cl}$ in a near-cathode layer, including the sheath, on a W cathode of radius $R = 2$ mm and height $h = 10$ mm in atmospheric-pressure Ar arc shown in figure 1. These data have been calculated by means of the free Internet tool [23], which is based on the sheath-accounted approach and allows one to calculate the diffuse and axially symmetric spot modes of current transfer to rod cathodes in arc plasmas of different compositions; the data shown in figure 1 refer to the diffuse mode. The current–voltage characteristic

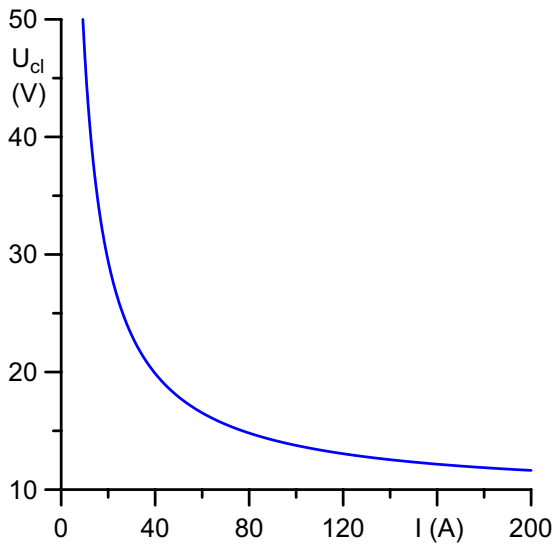


**Figure 1.** Cathode fall on a rod W cathode in an atmospheric-pressure Ar plasma; cathode radius 2 mm, height 10 mm. Simulations by means of the Internet tool [23].

falls; however, the near-cathode voltage even in the range of high currents, $I = 100$–$200$ A, is still between 13.8 and 11.6 V. A bit higher value $U_{\rm cl} = 15$ V can be deduced from the graphs of [15]; this value refers to the cathode fall at the centre of a W cathode with $R = 10$ mm and $h = 8$ mm in an atmospheric-pressure Ar arc at $I = 200$ A. These examples show that the cathode fall predicted by the sheath-accounted approach for high-current arcs is in the range 10–15 V, well in excess of 1–2 V assumed in the framework of the no-sheath approach.

Second, a still more general approach is the one in which a system of equations including the Poisson equation is solved throughout the whole near-cathode region in a straightforward way, without assuming the quasi-neutrality or an *a priori* division of the near-cathode region into a space-charge sheath and a quasi-neutral plasma. Such modelling [24] has shown that the sheath is of primary importance; regimes, where the sheath plays a minor role, are in principle possible, however, they do not occur under conditions of high-pressure arc discharges.

Thus, methodological considerations indicate that the near-cathode sheath in high-current arcs is of primary importance, thus supporting the sheath-accounted approach against the no-sheath one.

### *1.3. Sheath and quasi-neutral plasma voltages in high-current arcs*

An argument in favour of the LTE models of high-pressure high-current arc discharges is their ability to predict arc voltages that are not very different from experimental values. A possible interpretation is that the dominating contribution to the arc voltage is given by the arc column, which is in the state of LTE at high arc currents. This is difficult to reconcile with the presence of a near-cathode space-charge sheath with a significant voltage. This contradiction must be resolved before a definite conclusion on justifiability of the no-sheath versus sheath-accounted approaches can be reached.

It was found in [25] that the electric power deposited into the near-cathode sheath is transported not only to the cathode but also to the quasi-neutral plasma (arc column), an effect that cannot be described by LTE models. This effect has been independently confirmed in [24]. Obviously, this transport can substantially reduce the resistance of the part of the arc column adjacent to the sheath. In order to describe this transport, one needs to take into account not only the presence of the sheath, but also eventual discrepancy between the electron and heavy-particle temperatures $T_e$ and $T_h$ in the arc column, at least in the part adjacent to the near-cathode sheath. Both effects, which are discarded in LTE models, have been taken into account in [24, 25].

Thus, one may hypothesize that LTE models substantially overestimate the resistance of the part of the arc column that is adjacent to the near-cathode sheath and this overestimation to a certain extent compensates discarding the voltage in the near-cathode sheath. This question clearly deserves an elaboration. Another question that needs to be analysed is the effect of deviations from LTE on the resistance of the bulk of the arc column.

In this work, a model similar to that in [25] is employed for finding electrical characteristics of a high-current atmospheric-pressure argon arc. Also performed are simulations by means of an LTE model. The arc voltage predicted by both models is compared with the experimental data [26]. Also considered is the question of error introduced into the evaluation of the resistance of a near-cathode plasma by algorithms conventionally used in LTE models.

## 2. The model

The model used in this work is similar to the one of [25] and may be briefly described as follows. The whole system comprising the arc and the electrodes is divided into three sub-domains simulated by means of separate models: the cathode and the near-cathode plasma layer, the arc column, the anode; the near-anode plasma layer is discarded. The cathode and the near-cathode plasma layer are described by means of the model of nonlinear surface heating. A summary of equations of the model can be found in [27]. A more detailed description and an online tool for simulation of the diffuse and spot modes of current transfer and their stability based on this model can be found in [23]. Detailed presentations of different aspects of the model, as well as its detailed experimental validation, can be found in [13] and original works cited therein.

In brief, the model of nonlinear surface heating may be introduced as follows. The model exploits the following feature of the physical picture accounting for the existence of the sheath: the electrical energy deposited by the arc power supply in a sheath with a voltage of 10–15 V is quite significant, and it is a part of this energy that is transported to the cathode and heats it; as a consequence, the plasma–cathode interaction is governed by processes occurring in a thin near-cathode plasma layer comprising the sheath and the adjacent ionization layer, and to the first approximation the plasma–cathode interaction is unaffected by the arc column. In mathematical terms, the model of nonlinear surface heating involves the equation of heat conduction in the cathode body coupled through a boundary condition with a system of transcendental equations describing current transfer through the near-cathode layer. The motion of ions in the space-charge sheath is assumed to be collisionless and is described kinetically. (This description is expected to be reasonably accurate also in the case of moderately collisional sheaths, although not in the case where the ion motion in the sheath is strongly collisional, which occurs, for example, in very-high pressure high-intensity discharge lamps operating under the pressure of the order of 100 bar or higher.) The ionization layer is described by means of fluid equations. Calculation of distribution of potential in the cathode has shown that the variation of potential in the cathode does not exceed 0.4 V for conditions considered in this work, therefore the voltage drop and Joule heating in the cathode body are neglected. The voltage drop $U_{cl}$ across the near-cathode layer is assumed to be the same at different points of the arc attachment.

The arc column is computed by means of a two-temperature (2T) hydrodynamic model, which accounts for inequality of the electron and heavy-particle temperatures, $T_e \neq T_h$, but assumes the ionization equilibrium and quasi-neutrality. The model comprises the Navier–Stokes equations, equations of energy for the heavy particles and the electrons, equation of continuity of electric current supplemented with Ohm's law and Ampère's law for the self-induced magnetic field. The anode is simulated by means of a model comprising equations of heat conduction and continuity of electric current supplemented with Ohm's law. Note that variations of potential in the anode are in fact very small (of the order of 1 mV); however, the current continuity equation is nonetheless maintained in the model for technical reasons.

The coupling between the sub-domains is as follows. Let us use $T_h$ for the heavy-particle temperature, where the arc column and the near-cathode plasma layer are concerned, and for the temperature of the electrode material, where the electrodes are concerned. At the interface between the arc column and the near-cathode layer, the temperature $T_h$ is assumed to be continuous, as well as the electron temperature $T_e$, the electrostatic potential $\varphi$, and the normal component $j_n$ of the electric current density (here and further $n$ is a coordinate measured from the electrode surface normally to it in the direction into the plasma). Note that variations of heavy-particle temperature across the near-cathode layer are neglected; we recall that the near-cathode plasma layer, which is of interest for this work, comprises the sheath and the ionization layer and its thickness is of the order of 1 $\mu$m or smaller. Therefore, the continuity of $T_h$ means that the heavy-particle temperature on the arc column side of the interface equals the temperature of the cathode surface.

At the interface between the arc column and the anode, $T_h$, $\varphi$ and $j_n$ are assumed to be continuous. The density of flux of energy from the arc column to the anode is evaluated as the sum of heat fluxes transported by the heavy particles and the electrons and of the additional term $j_n(A_f + 2.5kT_e)/e$ (here $A_f$ is the work function of the electrode material), which accounts for heating of the anode surface due to condensation of electrons.

The model of nonlinear surface heating is implemented on the basis of COMSOL Multiphysics software, similarly to how it was done in [28]. The problems describing the arc column and the anode are solved jointly by means of a code based on the SIMPLE algorithm [29, 30], similarly to how it was done in [25]. While solving the problem for the arc column, the near-cathode layer is assumed to be infinitely thin and the interface between the arc column and the near-cathode layer is assumed to coincide with the cathode surface.

The calculation procedure is as follows. First, the model of nonlinear surface heating is run to obtain, for a given arc current $I$, the distribution of temperature inside the cathode and on its surface, the voltage drop $U_{\rm cl}$ in the near-cathode plasma layer, and the distribution of parameters of plasma in the near-cathode layer along the cathode surface. In particular, distributions are found of the temperature of the cathode surface, $T_{\rm h}(s)$, electron temperature in the near-cathode layer, $T_{\rm e}(s)$, and density of electric current from the near-cathode layer into the arc column, $j_{\rm n}(s)$. (Here $s$ is a coordinate measured along the electrode surface.) These distributions serve as boundary conditions at the interface between the near-cathode layer and the arc column for the equation of energy of heavy particles, the equation of energy of electrons and current continuity equation, which make part of the 2T hydrodynamic model of the arc column.

The above-described model will be referred to as the 2T-sheath model. Another model treated in this work is the LTE one. The LTE model differs from the 2T-sheath model in three aspects: it is assumed that $T_{\rm e} = T_{\rm h}$ in the arc column; the near-cathode layer is discarded; the cathode is simulated in the same way as the anode, i.e. by means of equations of heat conduction and continuity of electric current with the boundary conditions at the interface between the cathode and the arc column similar to those at the interface between the arc column and the anode. Note that since $T_{\rm e} = T_{\rm h}$ in the arc column, the additional term in the expression for the density of flux of energy from the plasma to the electrodes is $j_{\rm n}(A_f + 2.5kT_{\rm h})/e$. (Since $j_{\rm n} < 0$ at the cathode, this term is negative as it should: electrons leaving the cathode cause cooling of the cathode surface rather than heating.) The boundary condition for the current continuity equation at the base of the cathode is a constant current density equal to $I/\pi R^2$, where $R$ is the cathode radius. The problems describing the arc column and both electrodes are solved jointly by means of a code based on the SIMPLE algorithm.

## 3. Numerical results

The geometry considered in this work corresponds to conditions of experiment [26] and is shown in figure 2. The arc chamber is closed (no gas pumping). The cathode is made of tungsten and represents a rod with a hemispherical tip. The anode is flat and made of copper. Boundary conditions at the outer boundaries of the computation domain are listed in table 1 and are conventional. Results reported in this work refer to the case $T_{\rm amb} = 300$ K and the arc current range 20–200 A.

Distributions of electrical parameters on the axis of the arc column for $I = 40$ A and $I = 160$ A computed by means of the 2T-sheath and LTE models are shown in figure 3. Since the

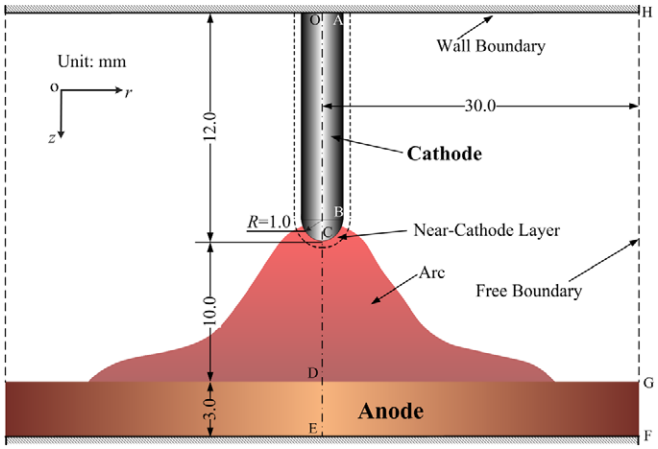


**Figure 2.** Calculation domain.

interface separating the arc column and the near-cathode layer in the framework of the 2T-sheath model is assumed to coincide with the cathode surface while the arc column is treated, the axis of the arc column occupies the range 12 mm $\leqslant z \leqslant$ 22 mm in both models.

In figure 4, distributions of the potential and the normal component of the current density over the interface separating the arc column and the near-cathode layer in the framework of the 2T-sheath model are shown. (Here $s$ is the distance from the centre of the front surface of the cathode (i.e. from point $C$ in figure 2) measured along the generatrix, distribution $j_{\rm n}(s)$ is given by the code describing the cathode and the near-cathode layer, distribution $\varphi(s)$ is given by the code describing the arc column and the anode.) One can see that the variation of $\varphi(s)$ in the region $s \lesssim 2$ mm, which is where the arc is present, is small (below 1 V). This result justifies the assumption that the voltage drop in the near-cathode layer, $U_{\rm cl}$, is approximately the same at all points of the cathode surface inside the arc attachment; this assumption is employed in this model and allows one to conveniently avoid iterations between the code describing the cathode and the near-cathode layer and the code describing the arc column and the anode.

Let us denote by $U_{\rm ac}^{\rm (2T)}$ and $U_{\rm ac}^{\rm (LTE)}$ the voltage drop over the axis of the arc column evaluated in the framework of, respectively, the 2T-sheath and LTE models. It follows from the preceding paragraph that the interface between the arc column and the near-cathode layer is approximately equipotential, hence the potential difference evaluated along the axis of the arc column, $U_{\rm ac}^{\rm (2T)}$, may be interpreted as the arc column voltage in the framework of the 2T-sheath model. $U_{\rm ac}^{\rm (LTE)}$ represents the arc column voltage in the framework of the LTE model. These voltages as functions of the arc current are shown in figure 5. Both increase with increasing current, however $U_{\rm ac}^{\rm (LTE)}$ is significantly higher than $U_{\rm ac}^{\rm (2T)}$.

The fact that the arc-column voltage predicted by the LTE model is significantly higher than that predicted by the 2T-sheath model is related to the axial electric field predicted by the LTE model being higher than that predicted by the 2T-sheath model virtually everywhere in the arc column, as seen in figure 3(*b*). (In the case $I = 160$ A, there is a region adjacent to the anode where the 2T-sheath model predicts a higher electric

**Table 1.** Boundary conditions at the outer boundary of the calculation domain.

| | OC | CD | DE | EF | FG | GH | HA | AO |
|---|---|---|---|---|---|---|---|---|
| $v_r$ | — | 0 | — | — | — | $\frac{\partial(\rho r v_r)}{\partial r} = 0$ | 0 | — |
| $v_z$ | — | $\frac{\partial v_z}{\partial r} = 0$ | — | — | — | $\frac{\partial v_z}{\partial r} = 0$ | 0 | — |
| $T_\mathrm{h}$ | $\frac{\partial T_\mathrm{h}}{\partial r} = 0$ | $\frac{\partial T_\mathrm{h}}{\partial r} = 0$ | $\frac{\partial T_\mathrm{h}}{\partial r} = 0$ | $T_\mathrm{amb}$ | $\frac{\partial T_\mathrm{h}}{\partial r} = 0$ | $\frac{\partial T_\mathrm{h}}{\partial r} = 0$, $v_r \geqslant 0$<br>$T_\mathrm{h} = T_\mathrm{amb}$, $v_r < 0$ | $T_\mathrm{amb}$ | $T_\mathrm{amb}$ |
| $T_\mathrm{e}$ | — | $\frac{\partial T_\mathrm{e}}{\partial r} = 0$ | — | — | — | $\frac{\partial T_\mathrm{e}}{\partial r} = 0$ | $\frac{\partial T_\mathrm{e}}{\partial z} = 0$ | — |
| $\varphi$ | — | $\frac{\partial \varphi}{\partial r} = 0$ | $\frac{\partial \varphi}{\partial r} = 0$ | 0 | $\frac{\partial \varphi}{\partial r} = 0$ | $\frac{\partial \varphi}{\partial r} = 0$ | $\frac{\partial \varphi}{\partial z} = 0$ | — |

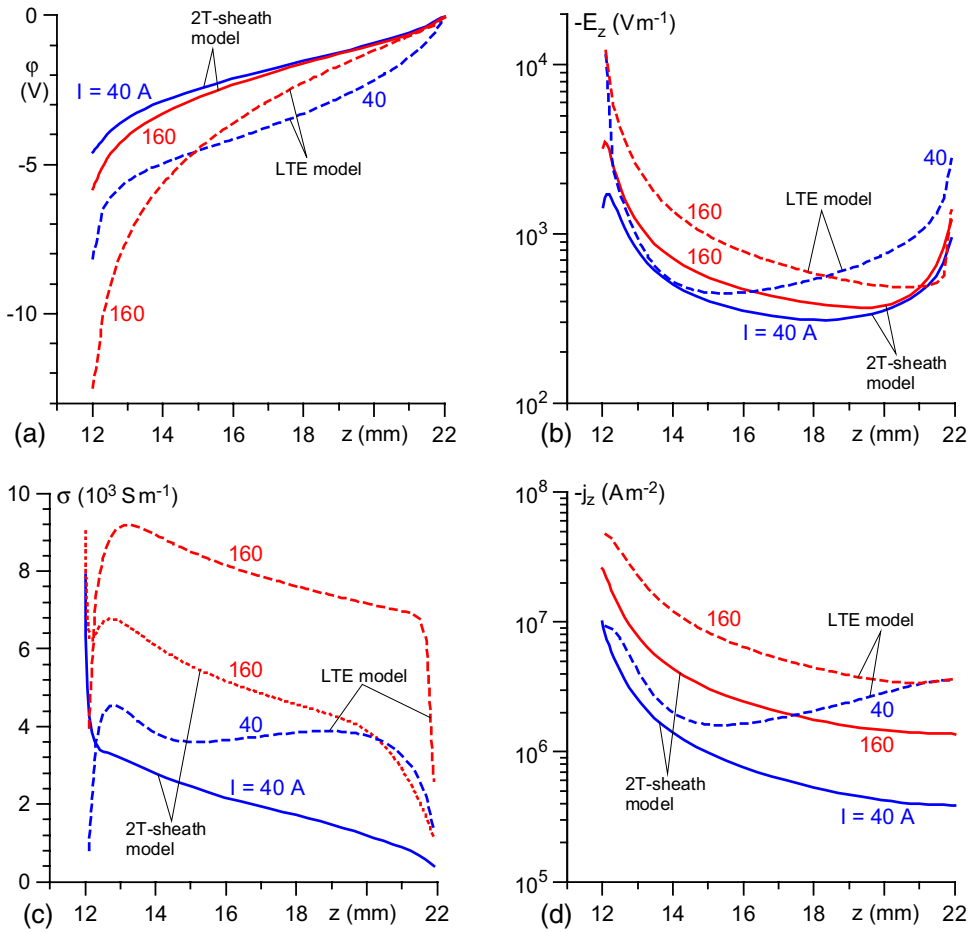


**Figure 3.** Distributions of electrical parameters on the axis of the arc column; $I = 40$, 160 A. (*a*) Electrostatic potential; (*b*) axial electric field and (*c*) electrical conductivity of the plasma. The data referring to the 2T-sheath model for $I = 160$ A are represented by a dotted line in order to distinguish in the black-and-white print from the line representing the data for $I = 40$ A. (*d*) Axial current density.

field; however, this region is narrow and unimportant for the following.)

As far as the bulk of the arc column is concerned, the reason for values of $|E_z|$ predicted by the LTE model being higher is as follows. In figure 6, radial distributions of parameters of the arc column in the midplane of the arc, $z = 17$ mm (i.e. halfway between the electrodes), are shown. In the framework of the 2T-sheath model, the electron temperature and, consequently, electrical conductivity of the plasma in the arc fringes are higher than those for the same $I$ in the framework of the LTE model. The current density is higher in the arc fringes and correspondingly lower in the arc core; the latter is seen also from figure 3(*d*). The temperature in the arc core is also lower. Thus, the arc core as described by the 2T-sheath model is colder and wider, hence the energy losses from it are lower. The latter means that the arc column consumes a lower electrical power, i.e. for the same arc current the axial electric field is lower.

There is an additional reason for values of $|E_z|$ predicted by the LTE model being higher which comes into play in the immediate vicinity of the cathode or, in the framework of the 2T-sheath model, of the interface separating the column from the near-cathode layer. This reason is seen from figure 3(*c*): $\sigma$ calculated by means of the LTE model rapidly decreases

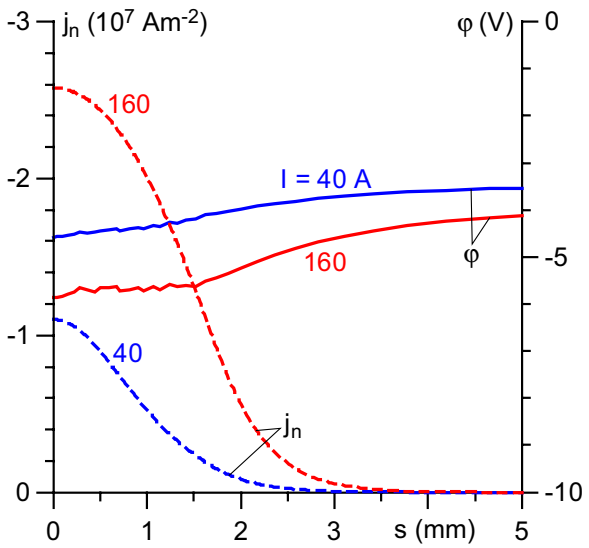


**Figure 4.** Distributions of potential and normal current density along the interface separating the arc column and the near-cathode layer; $I = 40$, 160 A.

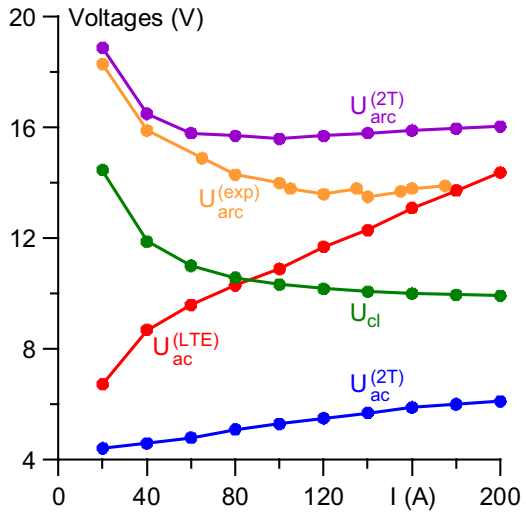


**Figure 5.** $U_{ac}^{(2T)}$, $U_{ac}^{(LTE)}$: arc column voltage evaluated by means of, respectively, the 2T-sheath and LTE models. $U_{cl}$, $U_{arc}^{(2T)} = U_{ac}^{(2T)} + U_{cl}$: voltage drop in the near-cathode layer and arc voltage evaluated by means of the 2T-sheath model. $U_{arc}^{(exp)}$: measured arc voltage [26].

in this vicinity, while $\sigma$ calculated by means of the 2T-sheath model rapidly increases. This is a consequence of different behaviour of the temperatures, which is shown in figure 7. Both the heavy-particle temperature $T_h$ and the LTE plasma temperature $T$ decrease in the direction to the cathode (note that at $z = 12$ mm both $T_h$ and $T$ equal the temperature of the cathode surface, which does not exceed 4000 K). However, the electron temperature $T_e$, which governs the plasma conductivity in the 2T-sheath model, increases, which is due to the transport into the arc column of electric power deposited into the near-cathode sheath [24, 25].

The total arc voltage in the framework of the 2T-sheath model, $U_{arc}^{(2T)}$, is obtained by adding the arc column voltage $U_{ac}^{(2T)}$ and the voltage drop in the near-cathode layer, $U_{cl}$. These voltages as functions of current are shown in figure 5. One can see that the arc column contributes about one-third or less of the arc voltage and the rest is contributed by the near-cathode layer, i.e. essentially by the space-charge sheath. $U_{arc}^{(2T)}(I)$ decreases for lower currents, passes through a minimum at $I = 100$ A, and slowly increases for higher currents.

Also shown in figure 5 are experimental data on the arc voltage, $U_{arc}^{(exp)}$, taken from [26]. (The authors [26] distinguish two forms of arc attachment to the cathode: diffuse and contracted. However, the difference between the corresponding arc voltages is below 1 V. We note for definiteness that the values shown in figure 5 refer to the diffuse form.) The dependence $U_{arc}^{(exp)}(I)$ is similar to $U_{arc}^{(2T)}(I)$, although the minimum occurs at a higher current $I = 140$ A. The numerical values are also not very different: $U_{arc}^{(2T)}$ exceeds $U_{arc}^{(exp)}$ by less than 1 V at lower currents and by about 2 V at higher currents.

In the framework of the LTE model, the total arc voltage coincides with the arc column voltage $U_{ac}^{(LTE)}$. The dependence $U_{ac}^{(LTE)}(I)$ is of a different character than $U_{arc}^{(2T)}(I)$ and $U_{arc}^{(exp)}$: $U_{ac}^{(LTE)}(I)$ monotonically increases for all currents. $U_{ac}^{(LTE)}$ is lower than both $U_{arc}^{(2T)}$ and $U_{arc}^{(exp)}$; the difference is significant for lower currents but decreases with current and is reduced to no more than approximately 2 V for $I \gtrsim 120$ A.

## 4. Effect of numerics over the arc voltage predicted by the LTE model

Sensitivity with respect to details of numerical grids in the vicinity of the cathode is a known issue for LTE models of high-pressure arc discharges. In this connection, computations have been performed in which the code describing the arc column and the anode (and, in the case of the LTE model, also the cathode) was operated on a series of grids successively refined in the vicinity of the cathode. The number of control volumes on the axis of the arc column in each of the grids and positions ($z$-coordinates) of the two main grid points, i.e. centres of control volumes closest to the cathode are indicated in table 2. Note that the simulations described in section 3 have been performed on grid 1 for the 2T-sheath model and on grid 4 for the LTE model.

An example of the results is shown in figure 8. One can see from figure 8($a$) that the use of different grids does not appreciably affect the results given by the 2T-sheath model.

In contrast, results given by the LTE model indeed depend on the grid, especially in the vicinity of the cathode. This effect is clearly seen in figure 8($b$), which represents a magnification of the relevant part of figure 8($a$), and is non-negligible. There is no way to eliminate this dependence by means of a further refinement of the grid in the vicinity of the cathode, since such refinement leads to the loss of convergence. The reason for the problem is well known: it is a steep decrease of the LTE plasma temperature in the vicinity of the cathode, which causes a dramatic variation of the plasma conductivity. The latter is illustrated by table 3. Here, indices $w$, 1 and 2 are attributed to values of the corresponding quantities at, respectively, the centre of the front surface of the cathode (point $C$ in figure 2) and the first and second main points of each grid on the axis

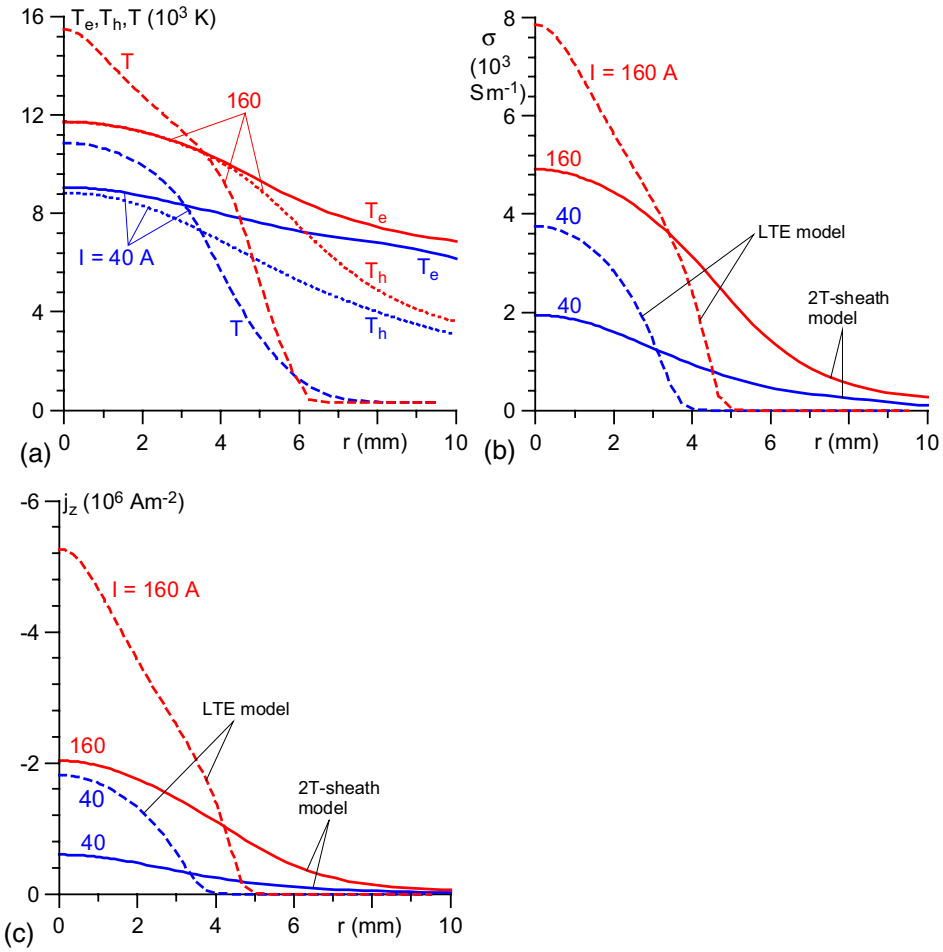


**Figure 6.** Radial distributions of parameters of the arc column in the midplane of the arc. $I = 40$, 160 A. (*a*) $T_e$, $T_h$: electron and heavy-particle temperatures (2T-sheath model), $T$: the plasma temperature (LTE model). (*b*) Electrical conductivity of the plasma. (*c*) Axial current density.

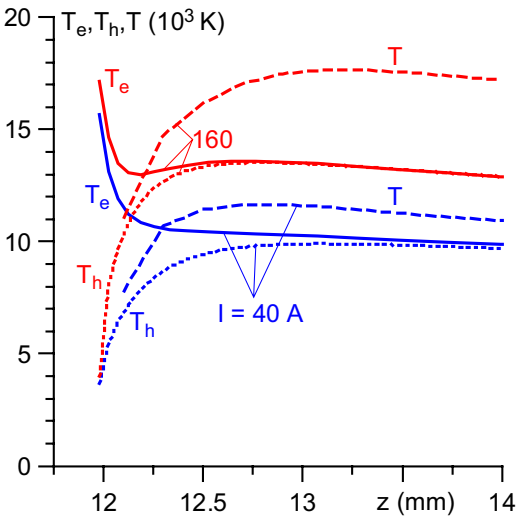


**Figure 7.** Axial distributions of electron and heavy-particle temperatures ($T_e$, $T_h$, 2T-sheath model) and of the plasma temperature ($T$, LTE model) in the arc column in the vicinity of the cathode surface; $I = 40$, 160 A.

of the arc (positions of these points are given in table 2); $T_w$ and $\varphi_w$ are determined by means of linear extrapolation of distributions of the temperature and potential at the axis of the cathode (note that the values of $U_{ac}^{(LTE)}$ shown in figure 5 and the values of potential at $z = 12$ mm shown in figure 8(*b*) are also determined in this way); $\sigma_w$ is evaluated in terms of $T_w$ by means of the data [31]. There is a two- to five-fold variation of $\sigma$ between the second and first main grid points and a variation of five orders of magnitude between the first main grid point and the cathode surface.

In the SIMPLE numerical algorithm being used, transport coefficients are assumed to be constant in each control volume; an assumption clearly unsuitable as far the electrical conductivity of the plasma near the cathode is concerned. Note that transport coefficients on the interface between adjacent control volumes are evaluated as a harmonic mean value (e.g. [30, 32]) in the SIMPLE algorithm. Therefore, the plasma conductivity at the cathode surface is assumed to be equal to roughly twice the value at the centre of the first control volume in the plasma, which represents a further deviation from reality.

Let us investigate this question in some detail. Let us consider the potential difference between the first main grid point on the arc axis, ($r = 0, z = z_1$), and the centre of the

**Table 2.** Characteristics of numerical grids used: number of control volumes on the axis of the arc column and positions of the two main grid points closest to the cathode.

| Grid | 1 | 2 | 3 | 4 | 5 | 6 | 7 |
|---|---|---|---|---|---|---|---|
| Model | 2T-sheath | | | LTE | | | |
| Number of points | 40 | 65 | 80 | 50 | 55 | 62 | 70 |
| $z_1$ (mm) | 12.022 | 12.020 | 12.008 | 12.100 | 12.060 | 12.035 | 12.022 |
| $z_2$ (mm) | 12.070 | 12.062 | 12.025 | 12.300 | 12.181 | 12.106 | 12.065 |

front surface of the cathode, ($r = 0, z = z_w$):

$$\varphi_1 - \varphi_w = -\int_{z_w}^{z_1} \frac{j_z}{\sigma}\,\mathrm{d}z. \tag{1}$$

In order to evaluate integral (1) numerically, one needs to interpolate the integrand on the interval $[z_w, z_1]$. A linear interpolation can be used for $j_z$:

$$j_z = j_z^{(w)} + \left(j_z^{(1)} - j_z^{(w)}\right) x, \qquad x = \frac{z - z_w}{z_1 - z_w}. \tag{2}$$

However, a linear, or any algebraic, interpolation would be inappropriate for $\sigma$, given its Arrhenius dependence on the plasma temperature and a strong variation of the latter in the vicinity of the cathode surface. It seems natural to approximate $\sigma$ by an Arrhenius function of the temperature (i.e. to assume that $\ln\sigma$ is a linear function of $-1/T$ in this interval) and to employ a linear interpolation of the temperature. The resulting interpolation reads

$$\sigma = \sigma_w \exp\left[\frac{a}{1 - t_w}\left(1 - \frac{t_w}{t}\right)\right], \tag{3}$$

$$t = t_w + (1 - t_w)\, x, \tag{4}$$

where $t = T/T_1$, $t_w = T_w/T_1$ and $a = \ln(\sigma_1/\sigma_w)$. Equation (1) assumes the form

$$\varphi_1 - \varphi_w = -\frac{j_z^{(w)}\,(z_1 - z_w)}{\sigma_w} b, \tag{5}$$

$$b = \int_0^1 (1 + cx) \exp\left[-\frac{ax}{t_w + (1 - t_w)\, x}\right] \mathrm{d}x, \tag{6}$$

where $c = j_z^{(1)}/j_z^{(w)} - 1$.

One can simplify equation (6) by exploiting the inequality $\sigma_w \ll \sigma_1$. By introducing a new integration variable, which coincides with the fraction in the exponent, one obtains

$$b = a t_w \int_0^a \frac{a + (c t_w - 1 + t_w)\, y}{[a - (1 - t_w) y]^3} \mathrm{e}^{-y}\,\mathrm{d}y. \tag{7}$$

Setting $a \to \infty$, one finds that $b = t_w/a$. [The same result may be obtained by replacing the integrand in equation (6) by $\exp(-ax/t_w)$.] Equation (5) assumes the form

$$-\frac{\varphi_1 - \varphi_w}{z_1 - z_w} = j_z^{(w)} \frac{T_w}{\sigma_w T_1 \ln(\sigma_1/\sigma_w)}. \tag{8}$$

The quantity on the left-hand side (lhs) of equation (8) represents the average electric field on the interval $[z_w, z_1]$. Hence, the second multiplier on the rhs may be interpreted as an average resistivity $\bar\rho$ of the plasma in this interval. It is convenient to write

$$\frac{\bar\rho}{\rho_1} = \frac{T_w}{T_1}\frac{\sigma_1}{\sigma_w} \ln^{-1}\frac{\sigma_1}{\sigma_w}. \tag{9}$$

The lhs of this expression represents the ratio of the average resistivity of the adjacent to the cathode half of the first control volume to the resistivity at the centre of the control volume.

It is seen from table 3 that $T_w/T_1$ and $\sigma_1/\sigma_w$ exceed, respectively, 0.35 and $5 \times 10^4$ for all grids. It follows from equation (9) that $\bar\rho/\rho_1$ exceeds 1500. Thus, the assumption of constant plasma conductivity in the first control volume results in underestimating the resistance of the half-volume adjacent to the cathode by a factor of more than 1500.

The above may be summarized as follows. As seen from table 3, the LTE model predicts for $I = 100$ A the potential difference $\varphi_1 - \varphi_w$, i.e. the voltage drop in the adjacent to the cathode half of the first control volume, of around 1 V. It is worth noting that this value does not vary significantly between different grids, although the distance over which this potential difference occurs, $z_1 - z_w$, varies very considerably: from 100 to 22 $\mu$m. The LTE model used in this work employs the assumption of plasma conductivity being constant within a control volume, which is usual in the SIMPLE numerical algorithm. If, however, one re-evaluates the potential difference $\varphi_1 - \varphi_w$ with the use of values of $j_z$ and $T$ from the converged LTE solution but with account of variation of $\sigma$, then $\varphi_1 - \varphi_w$ would amount not to 1 V but to more than 1.5 kV.

The procedure employed above for derivation of equation (8) is consistent with the mathematical technique of evaluation of integrals of exponential functions of a large argument. Note that if, for example, the linear interpolation is applied to $\sigma$ rather than to the plasma temperature, then one will obtain $\bar\rho/\rho_1 = \ln(\sigma_1/\sigma_w)$; a result incorrect by orders of magnitude.

## 5. Concluding remarks

The voltage over a 1 cm-long free-burning atmospheric-pressure argon arc, predicted by the 2T-sheath model, exhibits a variation with the arc current similar to the one revealed by the experiment and exceeds the experimental values by no more than approximately 2 V in the current range 20–175 A. About two-thirds or more of the arc voltage is contributed by the near-cathode sheath.

The model being employed describes the current transfer through the near-anode plasma layer in a rather crude way. More accurate models [33–35] indicate that the potential on

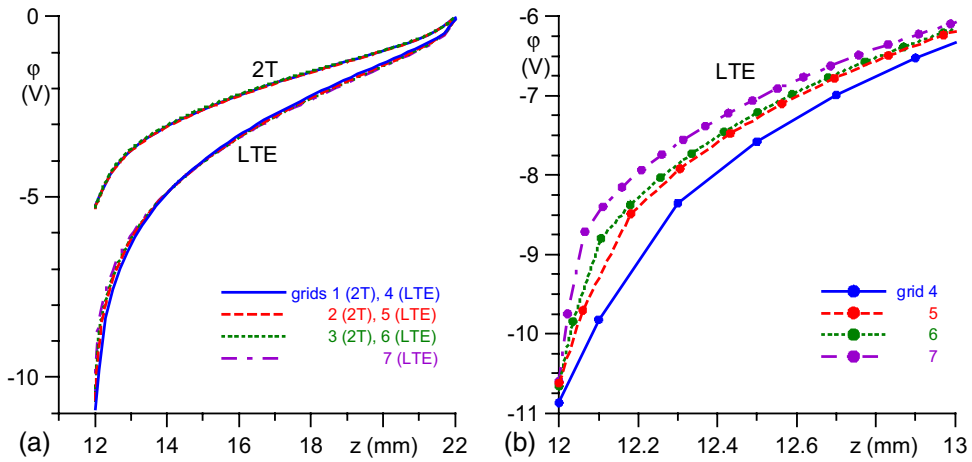


**Figure 8.** Distribution of potential on the axis of the arc column calculated on different grids; $I = 100$ A.

**Table 3.** Plasma temperature, conductivity, potential and axial current density at the centre of the front surface of the cathode and at the first and second main grid points on the arc axis obtained by means of LTE modelling on different grids; $I = 100$ A.

| Grid | 1 | 2 | 3 | 4 |
|---|---|---|---|---|
| $T_w$ (K) | 3688 | 3660 | 3659 | 3657 |
| $T_1$ (K) | 10 004 | 8915 | 8165 | 7389 |
| $T_2$ (K) | 13 113 | 11901 | 10 933 | 9652 |
| $\sigma_w$ (S m$^{-1}$) | $1.03 \times 10^{-2}$ | $8.82 \times 10^{-3}$ | $8.77 \times 10^{-3}$ | $8.67 \times 10^{-3}$ |
| $\sigma_1$ (S m$^{-1}$) | $2.89 \times 10^{3}$ | $1.80 \times 10^{3}$ | $1.10 \times 10^{3}$ | $5.20 \times 10^{2}$ |
| $\sigma_2$ (S m$^{-1}$) | $5.94 \times 10^{3}$ | $4.76 \times 10^{3}$ | $3.82 \times 10^{3}$ | $2.53 \times 10^{3}$ |
| $\varphi_w$ (V) | −10.87 | −10.62 | −10.66 | −10.60 |
| $\varphi_1$ (V) | −9.82 | −9.70 | −9.84 | −9.75 |
| $\varphi_2$ (V) | −8.35 | −8.49 | −8.80 | −8.71 |
| $j_z^{(w)}$ ($10^7$ A m$^{-2}$) | −3.12 | −2.85 | −2.60 | −2.13 |
| $j_z^{(1)}$ ($10^7$ A m$^{-2}$) | −2.91 | −2.64 | −2.47 | −2.00 |
| $j_z^{(2)}$ ($10^7$ A m$^{-2}$) | −2.58 | −2.41 | −2.42 | −2.00 |

the plasma side of the near-anode layer may exceed the anode potential by 1 or 2 V; the so-called negative anode fall. This may explain the above-mentioned deviation of up to about 2 V between the modelling and the experiment.

The LTE model predicts a different variation of the arc voltage with $I$ and underestimates the experimental values appreciably for low currents but by no more than approximately 2 V for $I \gtrsim 120$ A. The latter conforms to the well-known fact that LTE models of high-pressure arc discharges predict arc voltages which for high currents are close to experimental values. However, the present modelling suggests that this can hardly be considered as a proof of unimportance of the space-charge sheath: the LTE model overestimates both the resistance of the bulk of the arc column and the resistance of the part of the column that is adjacent to the cathode, and this overestimation to a certain extent compensates for the neglect of the voltage drop in the near-cathode sheath.

An extremely high resistivity of the near-electrode plasma is a known issue for LTE models of high-pressure arc discharges. If the potential difference between the first main grid point on the arc axis and the cathode is evaluated in terms of values of $j_z$ and $T$ taken from the LTE modelling but with a due account of the dramatic variation of $\sigma$, which occurs in the vicinity of the cathode, then the potential difference will be in excess of 1.5 kV. However, conventional numerical algorithms employed in the LTE modelling perform this evaluation in an inaccurate way and this inaccuracy amounts to a cut-off.

Obviously, some cut-off or other is in place in such a situation given the violation of the LTE in the vicinity of the cathode; at the end, switching from the arc-column equations to the sheath equations in the 2T-sheath model also can be viewed as a kind of cut-off. The difference is that the cut-off in numerical algorithms employed in the LTE modelling is of a numerical nature and does not reflect the physics of deviations from LTE occurring near the cathode. Therefore, the fact that this cut-off allows one to obtain arc voltages close to experimental values for high currents but not for low currents can hardly have physical meaning.

There are two-dimensional simulations of high-pressure arcs disregarding the sheaths but accounting for deviations from LTE due to ambipolar diffusion (e.g. [2, 3, 36, 37]) and due to both ambipolar diffusion and deviation between the electron and heavy-particle temperatures (e.g. [38, 39]). Inclusion of diffusion currents at the electrodes overcomes the problem of electrical conductivity at the electrodes being almost zero, existing in the LTE models. An analysis of this approach in light of the results of this work is a relevant task, however, falls beyond the scope of this paper.

## Acknowledgments

The work was supported by FCT-Fundação para a Ciência e a Tecnologia of Portugal through projects PTDC/FIS/68609/2006 and PEst-OE/MAT/UI0219/2011 and by the Natural Science Foundation of China through projects 11035005 and 10972119. The authors are grateful to J J Lowke, A B Murphy, and S M Shkol'nik for stimulating discussions. MSB gratefully acknowledges a visiting scientist grant from the Tsinghua University.

## References

[1] Gleizes A, Gonzalez J J and Freton P 2005 *J. Phys. D: Appl. Phys.* **38** R153
[2] Flesch P and Neiger M 2005 *J. Phys. D: Appl. Phys.* **38** 3098
[3] Lowke J J and Tanaka M 2006 *J. Phys. D: Appl. Phys.* **39** 3634
[4] Flesch P 2006 Light and light sources *High-Intensity Discharge Lamps* (Berlin: Springer)
[5] Murphy A B, Tanaka M, Tashiro S, Sato T and Lowke J J 2009 *J. Phys. D: Appl. Phys.* **42** 115205
[6] Schnick M, Fuessel U, Hertel M, Haessler M, Spille-Kohoff A and Murphy A B 2010 *J. Phys. D: Appl. Phys.* **43** 434008
[7] Tanaka M, Yamamoto K, Tashiro S, Nakata K, Yamamoto E, Yamazaki K, Suzuki K, Murphy A B and Lowke J J 2010 *J. Phys. D: Appl. Phys.* **43** 434009
[8] Tang K M, Yan J D, Chapman C and Fang M T C 2010 *J. Phys. D: Appl. Phys.* **43** 345201
[9] Murphy A B 2011 *J. Phys. D: Appl. Phys.* **44** 194009
[10] Ogino Y, Hirata Y and Nomura K 2011 *J. Phys. D: Appl. Phys.* **44** 215202
[11] Colombo V, Ghedini E, Boselli M, Sanibondi P and Concetti A 2011 *J. Phys. D: Appl. Phys.* **44** 194005
[12] Lebouvier A, Delalondre C, Fresnet F, Cauneau F and Fulcheri L 2012 *J. Phys. D: Appl. Phys.* **45** 025204
[13] Benilov M S 2008 *J. Phys. D: Appl. Phys.* **41** 144001
[14] Cayla F, Freton P and Gonzalez J-J 2008 *IEEE Trans. Plasma. Sci.* **36** 1944
[15] Gonzalez J J, Cayla F, Freton P and Teulet P 2009 *J. Phys. D: Appl. Phys.* **42** 145204
[16] Bergner A, Westermeier M, Ruhrmann C, Awakowicz P and Mentel J 2011 *J. Phys. D: Appl. Phys.* **44** 505203
[17] Dabringhausen L, Nandelstädt D, Luhmann J and Mentel J 2002 *J. Phys. D: Appl. Phys.* **35** 1621
[18] Luhmann J, Lichtenberg S, Langenscheidt O, Benilov M S and Mentel J 2002 *J. Phys. D: Appl. Phys.* **35** 1631
[19] Nandelstädt D, Redwitz M, Dabringhausen L, Luhmann J, Lichtenberg S and Mentel J 2002 *J. Phys. D: Appl. Phys.* **35** 1639
[20] Reinelt J, Westermeier M, Ruhrmann C, Bergner A, Awakowicz P and Mentel J 2011 *J. Phys. D: Appl. Phys.* **44** 095204
[21] Dabringhausen L, Langenscheidt O, Lichtenberg S, Redwitz M and Mentel J 2005 *J. Phys. D: Appl. Phys.* **38** 3128
[22] Zhukov M F, Kozlov N P, Pustogarov A V, An'shakov A S, Khvesyuk V I, Dyuzhev G A and Dandaron G-N B 1982 *Near-Electrode Processes in Arc Discharges* (Novosibirsk: Nauka) (in Russian)
[23] Benilov M S *et al* 2005 *Interaction of High-Pressure Arc Plasmas with Thermionic Cathodes* http://www.arc_cathode.uma.pt
[24] Almeida N A, Benilov M S and Naidis G V 2008 *J. Phys. D: Appl. Phys.* **41** 245201
[25] Li H-P and Benilov M S 2007 *J. Phys. D: Appl. Phys.* **40** 2010
[26] Mitrofanov N K and Shkol'nik S M 2007 *Tech. Phys.* **52** 711
[27] Benilov M S, Cunha M D and Naidis G V 2005 *Plasma Sources Sci. Technol.* **14** 517
[28] Benilov M S, Carpaij M and Cunha M D 2006 *J. Phys. D: Appl. Phys.* **39** 2124
[29] Zhu J 1991 Fast-2D: a computer program for numerical simulation of two-dimensional incompressible flows with complex boundaries *Report* No 690 Institute for Hydromechanics, University of Karlsruhe
[30] Patankar S V 1980 *Numerical Heat Transfer and Fluid Flow* (Washington: Hemisphere)
[31] Boulos M I, Fauchais P and Pfender E 1994 *Thermal Plasmas: Fundamentals and Applications* vol 1 (New York: Plenum)
[32] Date A W 2005 *Introduction to Computational Fluid Dynamics* (New York: Cambridge University Press)
[33] Nemchinskii V A and Perets L N 1977 *Sov. Phys. Tech. Phys.* **22** 1083
[34] Dinulescu H A and Pfender E 1980 *J. Appl. Phys.* **51** 3149
[35] Nazarenko I P and Panevin I G 1989 *Contrib. Plasma Phys.* **29** 251
[36] Fischer E 1987 *Philips J. Res.* **42** 58
[37] Sansonnens L, Haidar J and Lowke J J 2000 *J. Phys. D: Appl. Phys.* **33** 148
[38] Amakawa T, Jenista J, Heberlein J V R and Pfender E 1998 *J. Phys. D: Appl. Phys.* **31** 2826
[39] Haidar J 1999 *J. Phys. D: Appl. Phys.* **32** 263